



# Stability of Thermocapillary Flow in High-Prandtl-Number Liquid Bridges Exposed to a Coaxial Gas Stream

Mario Stojanovic<sup>1</sup> · Hendrik C. Kuhlmann<sup>1</sup>

Received: 8 April 2020 / Accepted: 23 July 2020 / Published online: 11 August 2020  
© The Author(s) 2020

## Abstract

The stability of thermocapillary flow in a liquid bridge made from 5 cSt silicone oil ( $Pr = 68$ ) is computed numerically. To improve the numerical model as compared to the standard approach, we consider the flow in the liquid bridge fully coupled to the flow in the ambient gas, temperature-dependent material parameters, and a dynamically deforming liquid–gas interface. We address the full two-phase-flow problem of interest for the space experiment JEREMI and investigate the effect of a steady axisymmetric coaxial gas flow which is imposed at the inlet of the annular gap between the liquid bridge and the outer confining cylinder. Under zero-gravity the flow is primarily driven by the imposed temperature gradient with viscous stresses from the gas phase being small. However, the heat transfer between liquid and the gas, and thus the temperature fields are strongly affected by the forced flow in the gas phase. As a result the stability of the steady axisymmetric flow depends sensitively on the flow direction and the temperature of the gas. If the temperature of the gas is identical to that of the support rod of the liquid bridge a gas stream opposing the thermocapillary stresses strongly destabilizes the basic flow. In a co-flow configuration the basic state is stabilized. Curves of neutral Reynolds numbers as functions of the strength of the annular gas flow are discussed for two aspect ratios of the liquid bridge.

**Keywords** Thermocapillary flow · Liquid bridge · Stability analysis · Two-phase flow · Heat transfer

## Introduction

The thermocapillary flow in liquid bridges and its stability have been widely studied as a fundamental model for crystal growth from the melt, see e.g. Cröll et al. (1991), Wanschura et al. (1997), and Leyboldt et al. (2000). Despite of all investigations, the heat transfer between the liquid bridge and the ambient gas is poorly understood and most difficult to control. In the past, most numerical studies addressed the problem considering only the liquid phase, neglecting viscous stresses from the gas phase and modeling

the heat transfer between liquid and gas by Newton's law (Nienhüser and Kuhlmann 2002; Wanschura et al. 1995). These assumption can lead to a poor numerical prediction of the real flow and its stability. Recent experiments revealed that the heat transfer across the interface strongly affects the stability boundaries of the axisymmetric steady flow (Yano et al. 2017). This observation has also been confirmed by numerical investigations (Shevtsova et al. 2014; Yasnou et al. 2018) which extended the computational domain into the gas phase and thus improved on the above mentioned approximations.

In the present work we consider a two-phase flow model which properly takes into account for a full mechanical and thermal coupling between the liquid and the gas phase. Moreover, our model allows for a dynamically deforming liquid–gas interface, its exact shape being part of the numerical solution. To this end, the Navier-Stokes, continuity and energy equations under zero gravity conditions are solved simultaneously for both, the liquid and the gas phase, coupled by the interfacial boundary conditions which involve the balance of normal and tangential stresses as well as the heat transfer between the two phases. Furthermore, temperature-dependent thermophysical properties of

---

This article belongs to the Topical Collection: The Effect of Gravity on Physical and Biological Phenomena  
Guest Editor: Valentina & Shevtsova

✉ Mario Stojanovic  
mario.stojanovic@tuwien.ac.at

Hendrik C. Kuhlmann  
hendrik.kuhlmann@tuwien.ac.at

<sup>1</sup> Institute of Fluid Mechanics and Heat Transfer, TU Wien, 1060, Vienna, Austria

both, the liquid and the gas phase are taken into account. To modify the liquid–gas heat transfer and to influence hydrodynamic instabilities an axisymmetric axial flow is imposed in the gas phase.

### Problem Formulation

A liquid bridge of length  $l_{lb}$  is kept in place by surface-tension forces between two concentric solid rods of radius  $r_i$ . The support cylinders with lengths  $l_{cold}$  and  $l_{hot}$  are mounted coaxially in a large cylindrical tube with radius  $r_o > r_i$  (Fig. 1). The rods are kept at different temperatures  $T_{cold} = T_0 - \Delta T/2$  and  $T_{hot} = T_0 + \Delta T/2$ , respectively, with constant mean temperature  $T_0 = 25^\circ\text{C}$ . Due to the temperature dependence of the surface tension  $\sigma(T) \approx \sigma_0(T_0) - \gamma(T - T_0)$ , where  $\gamma$  is the negative linear Taylor coefficient of the surface tension and the subscript 0 denotes the reference values, the fluid flow is driven by thermocapillary stresses along the liquid–gas interface. A gas stream with constant mean velocity  $\bar{w}^g$  is imposed in the annular gap surrounding the liquid bridge.

The symmetries of the problem allow for an axisymmetric and time-independent thermocapillary-driven basic flow. The basic flow is stably realized for sufficiently small temperature differences  $\Delta T$ . To properly take care of larger temperature differences the temperature dependence of the density  $\rho(T)$ , the specific heat capacity  $c_p(T)$ , the heat conductivity  $\lambda(T)$  and the dynamic viscosity  $\mu(T)$ , are taken into account in the governing equations. For this purpose the functional dependence of these material parameters are implemented according to the data sheet for Shin-Etsu silicone oils (Shin-Etsu 2004), the working fluid in the planned space experiment JEREMI (Shevtsova et al. 2014). The

steady state version of the continuity, Navier–Stokes and energy equations read

$$\nabla \cdot (\rho \mathbf{u}) = 0, \tag{1.a}$$

$$\nabla \cdot (\rho \mathbf{u} \mathbf{u}) = -\nabla p + \nabla \cdot \left\{ \mu \left[ \nabla \mathbf{u} + (\nabla \mathbf{u})^T \right] \right\}, \tag{1.b}$$

$$\nabla \cdot (\rho \mathbf{u} c_p T) = \nabla \cdot (\lambda \nabla T), \tag{1.c}$$

where  $\mathbf{u} = u\mathbf{e}_r + w\mathbf{e}_z$  is the axisymmetric velocity vector written in cylindrical coordinates,  $p$  the pressure and  $T$  the temperature field. Equations (1.1a–c) remain valid for the gaseous phase by simply considering the thermophysical properties of Argon ( $\rho^g, c_p^g, \lambda^g, \mu^g$ ), which is the foreseen working gas for the JEREMI experiment. The correlation equations for the temperature-dependent properties of argon are taken from VDI Wärmeatlas (2010). The properties of the liquid phase are denoted ( $\rho, c_p, \lambda, \mu$ ).

In addition to the usual no-slip conditions on all solid walls, we prescribe the fully developed annular velocity profile and the outflow condition  $\partial_z \mathbf{u} = 0$  at the inlet and at the outlet of the annular gap, respectively. While the outer cylinder is assumed adiabatic, the gas temperature at the inlet ( $z = 0$ ) and the outlet ( $z = l_{total} = l_{cold} + l_{lb} + l_{hot}$ ) are assumed to equal the respective temperatures of the cylindrical rods. On the axis at  $r = 0$  an axisymmetric flow requires

$$u = \partial_r w = \partial_r T = 0. \tag{2}$$

On the *a priori* unknown location of the liquid–gas interface, three kinds of boundary conditions have to be satisfied. The thermal boundary conditions

$$T = T^g \quad \text{and} \quad k \mathbf{n} \cdot \nabla T = k^g \mathbf{n} \cdot \nabla T^g \tag{3}$$

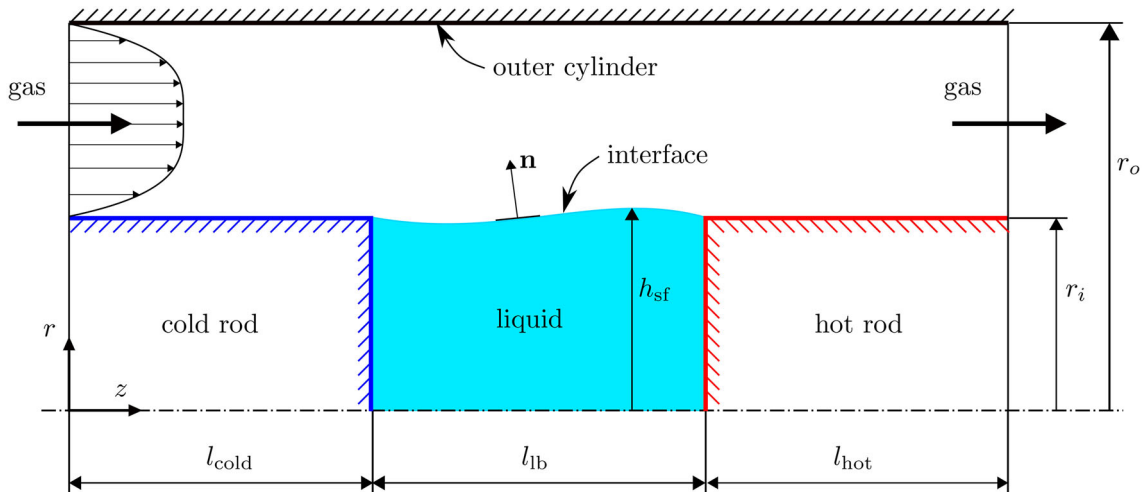


**Fig. 1** Computational domain: liquid and gaseous phase; dash-dotted line: axis of symmetry; radius of the rods:  $r_i$ , radius of the outer cylinder:  $r_o$ , length of the liquid bridge:  $l_{lb}$ , lengths of the cold and hot rod, respectively:  $l_{cold}$  and  $l_{hot}$

ensure continuity of the temperature and the heat flux across the interface, where  $\mathbf{n}$  is the outward-pointing unit normal vector to the interface. Here,  $k$  and  $k^g$  denote the heat conductivities of the liquid and of the gas, respectively. The kinematic boundary conditions

$$u = u^g, \quad w = w^g, \quad u/w = \partial_z h_{sf} \tag{4}$$

imply not only the no-slip condition at the interface, but also define the axisymmetric shape of the liquid bridge  $h_{sf}(z)$  to be a streamline. We consider the volume ratio

$$\mathcal{V} = \frac{\int_0^{l_{lb}} h_{sf}^2(s) ds}{r_i^2 l_{lb}} = 1, \tag{5}$$

which is the liquid volume normalized by the volume of the cylindrical gap between the two rods. The dynamic boundary condition

$$\mathbf{S} \cdot \mathbf{n} + \sigma (\nabla \cdot \mathbf{n}) \mathbf{n} - (\mathbf{I} - \mathbf{nn}) \cdot \nabla \sigma = \mathbf{S}^g \cdot \mathbf{n} \tag{6}$$

expresses the continuity of stresses, with  $\mathbf{I}$  being the identity matrix and  $\mathbf{S} = p\mathbf{I} + \mu [\nabla \mathbf{u} + (\nabla \mathbf{u})^T]$  the stress tensor (Kuhlmann 1999).

After solving the axisymmetric version of (1.b) – (1.c) simultaneously for both phases, coupled by the interface boundary conditions (3) – (6), we perform a linear stability analysis of the obtained solution (basic state). To this end the variables  $\mathbf{q} = (\mathbf{u}, p, T, \mathbf{u}^g, p^g, T^g)$  of the total flow

$$\mathbf{q} = \mathbf{q}_0(r, z) + \tilde{\mathbf{q}}(r, \varphi, z, t) \tag{7}$$

are decomposed into an axisymmetric part  $\mathbf{q}_0 = (\mathbf{u}_0, p_0, T_0, \mathbf{u}^g, p^g, T^g)$  and time-dependent three dimensional perturbations  $\tilde{\mathbf{q}} = (\tilde{\mathbf{u}}, \tilde{p}, \tilde{T}, \tilde{\mathbf{u}}^g, \tilde{p}^g, \tilde{T}^g)$ . Inserting ansatz (7) into the time-dependent three-dimensional version of (1.a-c), one obtains, after linearization with respect to the infinitesimal perturbations, a set of linear differential equations. This can be solved by the normal-mode ansatz

$$\tilde{\mathbf{q}} = \sum_{j,m} \hat{\mathbf{q}}_{j,m}(r, z) e^{\gamma_{j,m}t + im\varphi} + c.c., \tag{8}$$

resulting in an eigenvalue problem for the complex amplitudes  $\hat{\mathbf{q}}_{j,m}$ , where  $\gamma_{j,m}$  is the complex growth rate,  $m$  the azimuthal wave number and the index  $j$  numbers the discrete part of the spectrum. Varying the imposed temperature difference  $\Delta T$  between the two rods, one can find a solution  $\hat{\mathbf{q}}_{j,m}$  with  $\max_{j,m} \Re(\gamma_{j,m}) = 0$ . The corresponding critical temperature difference  $\Delta T_c$  is of key interest to our investigation.

Due to the temperature dependence of the thermophysical properties, one cannot take advantage of reformulating the governing equations including the boundary conditions in non-dimensional form. Thus, we solve all equations in

**Table 1** Geometrical parameters. All dimensions are given in mm

$l_{\text{cold}}$	$l_{\text{lb}}$	$l_{\text{hot}}$	$r_i$	$r_o$
5	{5; 9}	5	5	15

dimensional form and compute the critical thermocapillary Reynolds number

$$\text{Re}_c = \frac{\gamma l_{lb} \Delta T_c}{\mu_0^2 / \rho_0} \tag{9}$$

*a posteriori*. The dimensions of the geometry are given in Table 1. In the planned space experiment, the distance  $l_{lb}$  between the two rods will be adjustable such that different aspect ratios  $\Gamma = l_{lb}/r_i$  can be realized. In this study we focus on two aspect ratios  $\Gamma = 1$  and  $\Gamma = 1.8$ .

### Numerical Methods and Code Verification

The governing set of equations is discretized using second-order finite volumes on a staggered grid. A structured mesh with approximately 100.000 cells is used with a hyperbolic-tangent type of refinement towards all boundaries (Thompson et al. 1985). In order to resolve the thin thermal boundary layer occurring in high-Prandtl-number flows (Kuhlmann 1999) we choose a minimal cell size of  $\Delta_{\text{min}} = 5 \times 10^{-5} \times l_{lb}$  on all boundaries of the liquid bridge except for the axis of symmetry. Such a small cell size is required near the boundaries to obtain grid convergence. Furthermore, we introduce body-fitted coordinates  $(\xi, \eta)$

$$\xi = \frac{r}{h_{sf}} \quad \text{and} \quad \eta = \frac{z}{l_{\text{total}}}, \tag{10}$$

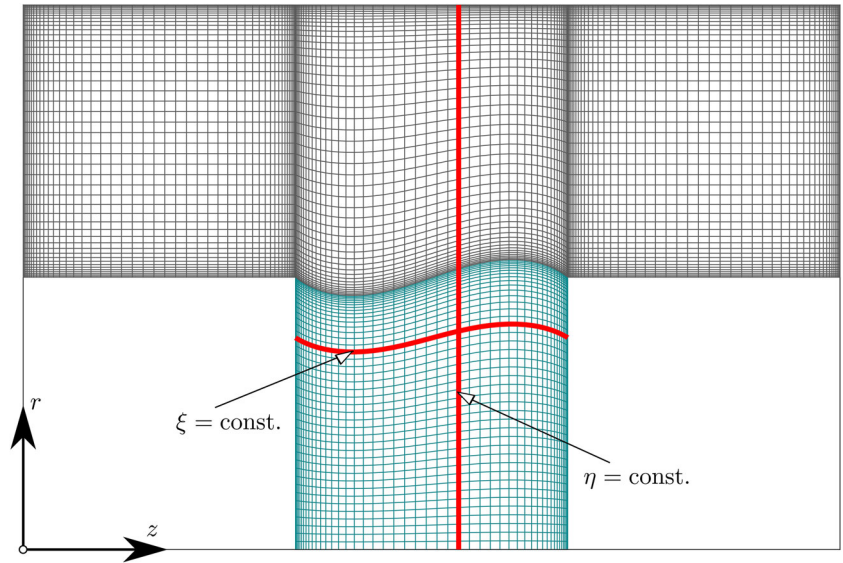
in order to map the computational domain for arbitrary interface shapes  $h_{sf}$  to a rectangular domain (see Fig. 2).

The resulting non-linear equations for the basic state are solved by the Newton-Raphson iteration. For the linear stability analysis the same discretization and solution methods are used.

Due to the lack of data in the literature for  $\text{Pr} = 68$ , the basic state obtained by our code for an indeformable interface has been compared by independent calculations of F. Romanò (private communication, see also Romanò et al. (2017)). All results compare very well qualitatively as well as quantitatively, even though both codes differ and different grids have been used.

To verify the flow-induced interface deformations  $h_{sf} - r_i$ , we have compared our results with the asymptotic solution of Kuhlmann and Nienhüser (2002) who provided explicit data for the thermocapillary low-Reynolds number flow with  $\text{Re} = 10^{-4}$  and  $\text{Pr} = 0.02$  (see Fig. 2 in

**Fig. 2** Example for the body-fitted computational grid



Kuhlmann and Nienhüser (2002)). An excellent agreement was found. It would also be interesting to further compare the shape of the liquid–gas interface with experimental measurements of Matsunaga et al. (2012) for an isothermal liquid bridge under normal gravity.

strength of the gas flow ( $\bar{w}^g l_{lb}$ ) for  $\Gamma = 1$ , where  $\bar{w}^g$  is the mean inlet velocity of the forced gas stream, i.e.

$$\bar{w}^g = \frac{2}{r_o^2 - r_i^2} \int_{r_i}^{r_o} w^g(r) \Big|_{z=0} r \, dr. \tag{11}$$

**Results**

Modes of neutral stability are found for different azimuthal wave numbers  $m$ . Figure 3 shows the corresponding neutral thermocapillary Reynolds numbers as function of the

As can be seen, the critical mode belongs to  $m = 1$  for the whole range of mean inlet velocities considered. While positive values on the abscissa denote a gas stream which opposes the thermocapillary stresses on the interface

**Fig. 3** Stability diagram for  $\Gamma = 1$ : Neutral and critical Reynolds numbers  $Re_c$  as functions of  $\bar{w}^g l_{lb}$ ; vertical dashed lines and yellow dots indicate reference values of the mean inlet gas velocity

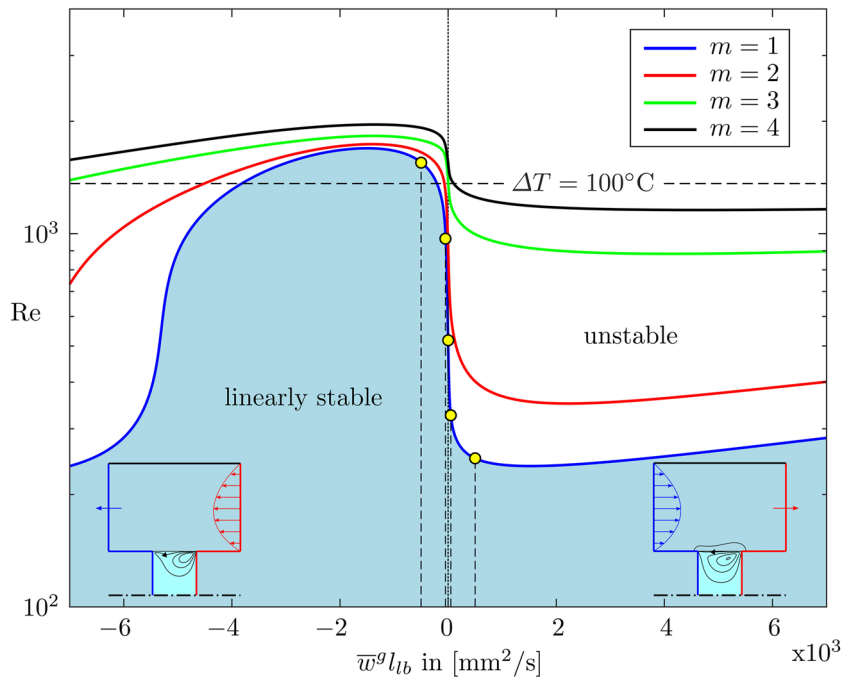
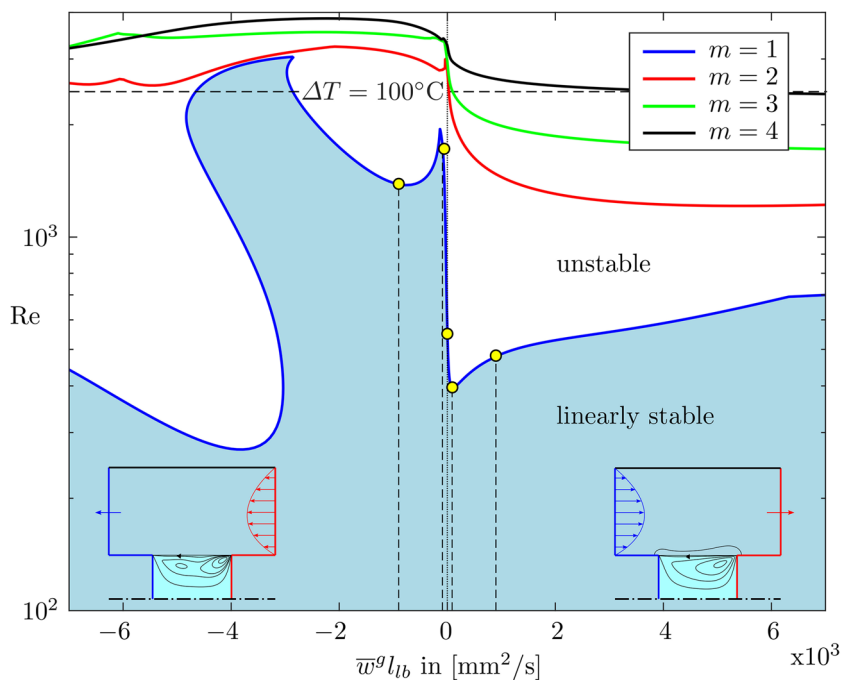


**Fig. 4** Stability diagram for  $\Gamma = 1.8$ : Neutral and critical Reynolds numbers  $Re_c$  as functions of  $\bar{w}^s l_b$ ; vertical dashed lines and yellow dots indicate reference values of the mean inlet gas velocity



(typically a counterflow situation), negative values indicate the gas flow is assisting thermocapillary stresses on the interface (typically a co-flow situation, inset in Fig. 3). Figure 3 reveals that co-flow of the gas has a stabilizing effect on the basic state: The critical Reynolds number sharply increases as  $\bar{w}^s l_b$  is decreased from zero. In contrast, positive mean inlet velocities (counter-flow) leads to a significant destabilization of the basic state, even for a weak gas flow. Note the Reynolds number in Fig. 3 is shown on a logarithmic scale. We find  $Re_c(\bar{w}^s = 0) = 527$  with a remarkable slope of  $\partial Re_c / \partial (\bar{w}_0^s l_b) |_{\bar{w}_0^s = 0} = 11 \text{ s/mm}^2$ .

The vertical dashed lines and yellow dots in Fig. 3 indicate the reference gas-flow velocities  $\bar{w}^s = \{0; \pm 10; \pm 100\} \text{ mm/s}$  for a comparison with future experiments. In order to relate the Reynolds number to the temperature difference  $\Delta T$  the horizontal dashed line marks a temperature difference of  $\Delta T = 100^\circ\text{C}$ . Such large temperature difference will be difficult if not impossible to achieve in experiments, because the correspondingly low  $T_{\text{cold}}$  in a normal environment may not be easily achievable and the associated high  $T_{\text{hot}}$  will result in a significant evaporation of the liquid, which is not considered in the present model. Hence, the onset of three-dimensional flow (in case the bifurcation is supercritical) will hardly be observable experimentally for  $\bar{w}^s = -100 \text{ mm/s}$ .

Neutral and critical Reynolds numbers for a longer liquid bridge with  $\Gamma = 1.8$  are shown in Fig. 4. Qualitatively, the behavior of  $Re$  for co- and counter-flow situations is comparable to the previous case, with  $m = 1$  again being the critical wave number. Neutral Reynolds numbers for larger wave numbers  $m > 1$  are relatively insensitive to the gas flow

rate. The critical curve (blue,  $m = 1$ ), however, exhibits sharp cusps. The critical mode changes discontinuously at the respective gas-flow rates.

### Discussion and Conclusion

All results presented have been obtained with our in-house code written in MATLAB. It has been extensively verified and validated. The code is capable of taking into account flow-induced surface deformations as well as temperature-dependent properties and is thus applicable in a wide range of flow parameters.

For both aspect ratios investigated, the neutral curves depend sensitively on the gas-flow direction. The forced gas flow has a significant stabilizing effect on the axisymmetric basic state if the gas stream is directed parallel to the thermocapillary stresses. In that case, the heat loss of the liquid phase to the gas phase through the free surface is reduced and may even be inverted such that the liquid becomes heated by the hot gas. In the counterflow configuration, on the other hand, the heat loss of the liquid phase to the gas through the free surface is enhanced, thus increasing temperature gradients in the liquid which leads to a destabilization of the basic flow.

Considering  $\Gamma = 1.8$ , there exist ranges of the gas flow rate, e.g. at  $\bar{w}^s l_b = -4000 \text{ mm}^2/\text{s}$ , at which we find three neutral Reynolds numbers. If the basic flow is destabilized at the lowest critical Reynolds number, it may possibly be re-stabilized at the middle neutral Reynolds number to again become unstable at the third (largest neutral

Reynolds number). Since the scenario will very much depend on the nonlinear behavior of the three-dimensional flow, it would be very interesting to investigate such case experimentally and numerically. Another interesting feature is the appearance of three cusps for of the critical curve for  $m = 1$ . These are absent for  $\Gamma = 1$ . These cusps are caused by changes of the critical mode. Therefore, an interesting nonlinear dynamics of the three-dimensional flow is expected near these parameters.

For a gas flow parallel to the thermocapillary stresses very high critical temperature differences are predicted by the current flow model. It would be interesting to investigate these parameters experimentally to validate our model for such extreme parameters. Most likely, for temperature differences of  $\Delta T_c = 100^\circ\text{C}$  or larger, other effects must be included in the numerical model. Candidates for such physical effects are evaporation of liquid (Simic-Stefani et al. 2006) and radiative heat exchange (Shitomi et al. 2019).

The critical Reynolds number is found to depend very sensitively on the gas flow rate near the limiting case of  $\bar{w}^s = 0$ . Therefore, in order to be able to compare with experiments, the experimental gas flow must be homogenous in the azimuthal direction  $\varphi$  and in time. Moreover, it is recommended to accurately determine the velocity profile  $w^s(r)$  of the gas flow at some stage  $z$  before reaching the liquid bridge.

Under zero gravity and in the absence of a forced gas flow the dynamic surface deformations are very small (Kuhlmann and Nienhüser 2002). The dynamic deformations due to the imposed gas flow, however, can reach up to 1% of  $r_i$  for the considered range of mean inlet velocities, depending on the gas flow rate and its direction. As expected, the deformations increase for an increasing aspect ratio  $\Gamma$ . When the dynamic surface deformation is taken into account in the basic state the critical Reynolds number changes by less than  $\pm 0.8\%$  compared to the case of a cylindrical interface. This change in  $\text{Re}_c$  is comparable to the magnitude of the shape change. However, the largest change of  $\text{Re}_c$  does not generally arise for the gas flow rate at which the dynamic interfacial deformation is largest.

Finally, we note that all results have been obtained for temperature-dependent material properties. This more accurate modeling is required to be able to predict the critical Reynolds number for the liquid bridges foreseen in the JEREMI experiment. These liquid bridges are relatively small and have a very high Prandtl number, thus a high viscosity. As a certain drawback, the results, in particular the critical Reynolds number, may depend on the size of the liquid bridge. The variation with temperature of the material properties can be disregarded thus facilitating the numerical modeling, if larger and less viscous liquid bridges are studied, because for a given critical Reynolds number

$\text{Re}_c$  the required temperature difference is much smaller, see (9).

**Acknowledgements** This work has been supported by FFG in the framework of ASAP14 under contract number 866027.

**Funding Information** Open access funding provided by TU Wien (TUW).

**Open Access** This article is licensed under a Creative Commons Attribution 4.0 International License, which permits use, sharing, adaptation, distribution and reproduction in any medium or format, as long as you give appropriate credit to the original author(s) and the source, provide a link to the Creative Commons licence, and indicate if changes were made. The images or other third party material in this article are included in the article's Creative Commons licence, unless indicated otherwise in a credit line to the material. If material is not included in the article's Creative Commons licence and your intended use is not permitted by statutory regulation or exceeds the permitted use, you will need to obtain permission directly from the copyright holder. To view a copy of this licence, visit <http://creativecommons.org/licenses/by/4.0/>.

## References

- Cröll, A., Müller-Sebert, W., Benz, K.W., Nitsche, R.: Natural and thermocapillary convection in partially confined silicon melt zones. *Microgravity Sci. Technol.* **3**, 204 (1991)
- Kuhlmann, H.C.: Thermocapillary Convection in Models of Crystal Growth Springer Tracts in Modern Physics, vol. 152. Springer, Berlin (1999)
- Kuhlmann, H.C., Nienhüser, C.: Dynamic free-surface deformations in thermocapillary liquid bridges. *Fluid Dyn. Res.* **31**, 103–127 (2002)
- Leyboldt, J., Kuhlmann, H.C., Rath, H.J.: Three-dimensional numerical simulation of thermocapillary flows in cylindrical liquid bridges. *J. Fluid Mech.* **414**, 285–314 (2000)
- Matsunaga, T., Mialdun, A., Nishino, K., Shevtsova, V.: Measurements of gas/oil free surface deformation caused by parallel gas flow. *Phys. Fluids* **24**, 062101 (2012)
- Nienhüser, C., Kuhlmann, H.C.: Stability of thermocapillary flows in non-cylindrical liquid bridges. *J. Fluid Mech.* **458**, 35–73 (2002)
- Romanò, F., Kuhlmann, H.C., Ishimura, M., Ueno, I.: Limit cycles for the motion of finite-size particles in axisymmetric thermocapillary flows in liquid bridges. *Phys. Fluids* **29**, 093303 (2017)
- Shevtsova, V., Gaponenko, Y., Kuhlmann, H.C., Lappa, M., Lukasser, M., Matsumoto, S., Mialdun, A., Montanero, J.M., Nishino, K., Ueno, I.: The JEREMI-project on thermocapillary convection in liquid bridges. Part b: Overview on impact of co-axial gas flow. *Fluid Dyn. Mat. Proc.* **10**, 197–240 (2014)
- Shin-Etsu: Silicone Fluid KF-96 – Performance test results. 6-1, Ohtemachi 2-chome, Chioda-ku, Tokyo, Japan (2004)
- Shitomi, N., Yano, T., Nishino, K.: Effect of radiative heat transfer on thermocapillary convection in long liquid bridges of high-Prandtl-number fluids in microgravity. *Int. J. Heat Mass Transf.* **133**, 405–415 (2019)
- Simic-Stefani, S., Kawaji, M., Yoda, S.: Onset of oscillatory thermocapillary convection in acetone liquid bridges: The effect of evaporation. *Int. J. Heat Mass Transfer* **49**, 3167–3179 (2006)
- Thompson, J.F., Warsi, Z.U., Mastin, C.W.: Numerical Grid Generation: Foundations and Applications. Elsevier North-Holland, Amsterdam (1985)

- VDI Wärmeatlas: 11th edn., VDI-Gesellschaft Verfahrenstechnik und Chemieingenieurwesen (GVC), Springer, Berlin, Heidelberg (2010)
- Wanschura, M., Kuhlmann, H.C., Rath, H.J.: Linear stability of two-dimensional combined buoyant-thermocapillary flow in cylindrical liquid bridges. *Phys. Rev. E* **55**, 7036–7042 (1997)
- Wanschura, M., Shevtsova, V.S., Kuhlmann, H.C., Rath, H.J.: Convective instability mechanisms in thermocapillary liquid bridges. *Phys. Fluids* **7**, 912–925 (1995)
- Yano, T., Nishino, K., Ueno, I., Matsumoto, S., Kamotani, Y.: Sensitivity of hydrothermal wave instability of Marangoni convection to the interfacial heat transfer in long liquid bridges of high Prandtl number fluids. *Phys. Fluids* **29**(4), 044105 (2017)
- Yasnou, V., Gaponenko, Y., Mialdun, A., Shevtsova, V.: Influence of a coaxial gas flow on the evolution of oscillatory states in a liquid bridge. *Int. J. Heat Mass Transfer* **123**, 747–759 (2018)

**Publisher's Note** Springer Nature remains neutral with regard to jurisdictional claims in published maps and institutional affiliations.